Jurnal Kejuruteraan 35(5) 2023: 1085-1100
https://doi.org/10.17576/jkukm-2023-35(5)-09

Optimize Process Parameter of FDM Techniques to Improve Mechanical Properties of Aerospace Application

Himat Rathod[a,b], Rishabh Makwana[b*] & Ghanshyam Acharya[b]

[a]*Gujarat Technological University. Ahmedabad, India*

[b]*Atmiya Institute of Technology & Science Rajkot, India*

**Corresponding author: rishabh.makwana@atmiyauni.ac.in*

Received 13 October 2022, Received in revised form 10 March 2023
Accepted 10 April 2023, Available online 30 September 2023

ABSTRACT

The Fused Deposition modelling technique is widely accepted by industries as it is the one of the most convenient modern technology. The fused deposition modelling (FDM) is one of the additive manufacturing techniques which are largely used for printing of metal/thermoplastic materials with ease of design flexibilities the proposed research had been carried out for the investigation and optimization of process parameters for product or application development through FDM. The FDM- (Fused deposition Modelling) is widely used for product development and do contain various control variables. Here the process relates to nozzle temperature, base plate temperature, filament feed, filament material and deposition speed. The research presented here had been conducted considering nozzle temperature, layer thickness, and internal profile as variables for specimen manufacturing. In Aerospace application, optimization process is highly required for the Properties of material, weight and other effects. Hence the tensile specimen had been prepared to represent an aerospace application of ducts for airflow. The full factorial design of experiments had been considered for experimental investigation. The design of experiment had been conducted with three factors; three no. of parameters at three different levels Hence, A total no. of 27 representation samples had been prepared for tensile test and surface roughness for the Optimum result. The results had given considerable parametric effect as an outcome. The optimized results had been manufactured on an Ultimaker3D printer machine and tested which confirmed the results. The outcomes will assure optimal manufacturing process parameters of FDM for improved mechanical properties.

Keywords: Additive Manufacturing, FDM Process, Acrylonitrile butadiene styrene (ABS) Material, Surface Roughness, Full Factorial Method, Tensile Strength

INTRODUCTION

Fused deposition modeling is an additive manufacturing process used to fabricate complex parts from CAD models. In this process, the parts are built from thin layers of extruded filaments of a semi-melted thermoplastic. The mechanical properties of FDM parts depend on variable factors such as the material's depositing orientation, filament's flow rate, raster's separation, and extrusion temperatures, etc. (Paleti, B et al. 2017).

Solid and shell are the two main FDM manufacturing strategies used indistinctively; however, there are a few applications where the solid build strategy may not be necessary and problematic. FDM process there is a nozzle that can movable in x-y direction onto a substrate deposits thread of molten polymeric material. The depth (i.e., Z direction) of the deposited material is adjusted by the table. The build material is heated slightly above (approximately 0.5° C) its melting temperature so that it solidifies within a very short time (approximately 0.1s) after extrusion and welds to the previous layer as shown in Figure 1.

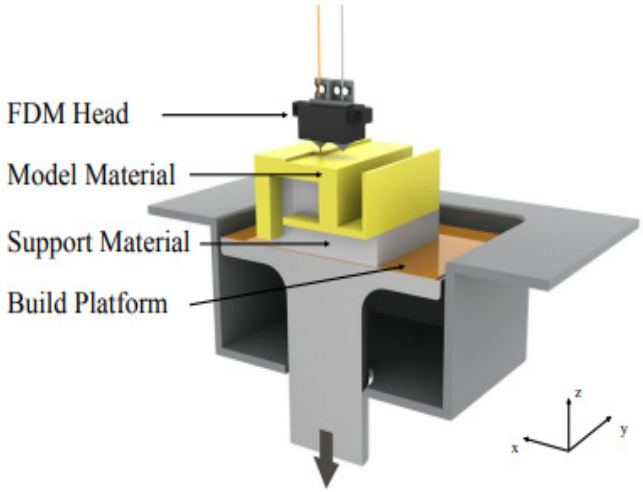

FIGURE 1. Fused Deposition Modeling Technology

Acrylonitrile Butadiene Styrene (ABS) is a specific type of plastic polymer made from the fusion of styrene and acrylonitrile with polybutadiene ABS is commonly used in the relatively new process of 3-D printing, where physical printers construct three-dimensional objects using programmed digital designs and models. (Paleti, B et al. 2017). Acrylonitrile butadiene styrene (ABS) (C8H8)x (C4H6)y (C3H3N)z is a common thermoplastic polymer. Its glass transition temperature is approximately 105 °C (221 °F). ABS is amorphous and therefore has no true melting point. The properties can fluctuate from 15 to 35% acrylonitrile, 5 to 30% butadiene, and 40 to 60% styrene. The outcome is a long chain of polybutadiene befuddled with shorter chains of poly (styrene-co-acrylonitrile). The nitrile bunches from neighboring chains, being polar, pull in one another and tie the chains together, making ABS more grounded than unadulterated polystyrene (Akessa et al. 2017). The styrene gives the plastic a glossy, impenetrable surface. Polybutadiene, a rubbery substance, gives strength even at low temperatures. For most uses, ABS can be utilized somewhere in the range of −20 and 80 °C (−4 and 176 °F) as its mechanical properties differ with temperature. The properties are made by elastic toughening, where fine particles of elastomer are dispersed all through the inflexible framework (Mohan et al. 2017)

LITERATURE REVIEW

(Paleti et al. 2017) explained about work the influence of the orientation and the mechanical data analyzed. Sample parts are generated with the given parameters of the native software based on the CAD data. First, specimens were analyzed concerning their geometry and configuration. The dimensions and weight were measured. The mechanical tests conducted were the tensile and compression tests.
Paleti, et al. 2017) given the study it can be observed) that solid structure has high compressive strength and high material used. Hollow internal structure has less fabrication time, low material used. Therefore, strength to weight ratio is required regarding less fabrication time. A solid internal structure is recommended weight is not .a critical factor

(Anoosha, et al. 2018) explained about the investigation is based on the maximum tensile test it found that 230◦ C temperature, 16 mm/s feed rate, and layer thickness are the optimum level building model in a different orientation, FEM analysis using ANSYS on tensile test the model 45◦ orientation has maximum tensile stress, a model built at 0◦ orientation and model built at 90◦ orientation has less tensile strength.

(Knoop et al. 2015) Investigations was conducted with the polymer Polyamide 12 (FDM Nylon 12) from Stratasys Inc. This polymer can be processed with layer thicknesses from 178 µm to 330 µm. Thus, the mechanical properties were determined for these layer thicknesses and different orientations on the build platform. In addition to the mechanical properties the thermal properties (e.g. with a DSC analysis) are also investigated.

(Bagsik et al. 2018) The influence of the orientation and the structure of the manufactured parts based on the mechanical data are analyzed. Sample parts are generated with the given parameters of the native software based on the CAD data. First, specimens were analyzed concerning their geometry and configuration. The dimensions and

weight were measured. The mechanical tests conducted were the tensile and compression tests.

Kovan et al. (2018) given a study of the effect of the surface roughens on layer thickness and the printing temperature of PLA. That printing parameter is very important in surface roughness, increasing layer thickness at printing temperature in an upright direction surface roughness value. The printing temperature lowers better surface quality.

Galantucci et al. (2015) investigation of research was to determine the impact of the sample's structure and building orientation on the tensile strength of 3D printed samples and thus to determine the combination that provides the highest strength. Test samples were prepared on a Z Corporation's 3D printer model Z310, with variations of internal geometrical structure, variations of longitudinal orientation, and also variations of base alignment.

Basavaraj et al. (2016) mainly focused discuss the process parameters for fused deposition modeling (FDM). Layer thickness, Orientation angle, and shell thickness are the study process variables.

An experiment done by Farbman et al. (2016) on the various mechanical properties of 3D printing material due to various factors many factors need to analyze when comes to predicting the strength of the 3D printing part. It's clear of the limited number and limited quality samples it's used the provide results. Components will want to know how to maximize the strength and durability of the product.

Three different topologies with similar relative densities were designed and fabricated by fused deposition modeling of ABS plus material. In the first stage, the material properties of the samples were evaluated and numerically correlated with experimental data. Experimental compression tests were performed on a universal strength machine. The comparison of the results of experiments and finite element analyses indicated acceptable similarity in terms of deformation, failure, and force characteristics. Additionally, a mesh sensitivity study was performed, and the influence of the mesh on the obtained results was assessed Kucewicz et al. (2018).

Joshi et al. (2015) investigates 3D printing is revolutionizing the world of manufacturing, even in the most advanced and sophisticated industries like the aerospace industry. This industry works around 2 basic principle requirements – low weight and high safety. 3D printing has been able to aid reduction in weight through complex and net shape manufacturing with less number of joints and intricate geometry. However, from the safety aspect, it is still a long way before being a reliable standard. Many challenges, such as printing patterns, porosity built-up, and uneven print flow, need to be solved and eliminated. It is just a matter of time. Once that happens, 3D printing would replace more and more traditional manufacturing techniques currently used in the aerospace industry and will have a sustained adaptation and growth.

Ngo et al. (2018) describes a different method, fused deposition modeling (FDM) is mainly used for fast prototyping, and the mechanical properties and quality of the printed parts are lower compared to the powder-bed methods such as selective laser sintering (SLS) and selective laser melting (SLM). Adjacent powders are fused, melted, or bonded together by using an auxiliary adhesive in Powder-bed methods, which result in finer resolutions but incur higher costs and are slower processes. However, it is a slow and complex procedure that is restricted by a limited number of materials. Finally, laminated object manufacturing (LOM) is based on layer-by-layer cutting and lamination of sheets or rolls of materials.

PROBLEM DEFINITION AND OBJECTIVES

PROBLEM DEFINITION

The internal structure is displayed utilizing the Full Factorial Method. The components of the example for testing are taken structure the ASTM D-638 standard shown in FIGURE fundamental components participated in a pattern to develop structure. FIGURE 2 (Paleti, et al. 2017) delineates the essential component of the internal structure.

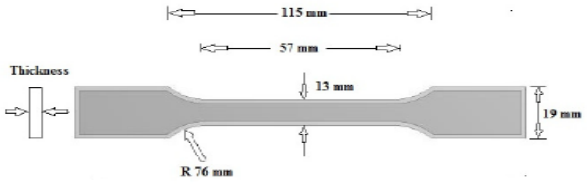

FIGURE 2. Parametric modeling of Internal structures

In the current work, three kinds of internal structures, for example, Tri-hexagon, Grid, and Concentric are viewed as which are appeared in FIGURE 3. These internal structures' reactions are contrasted and empty and strong cases.

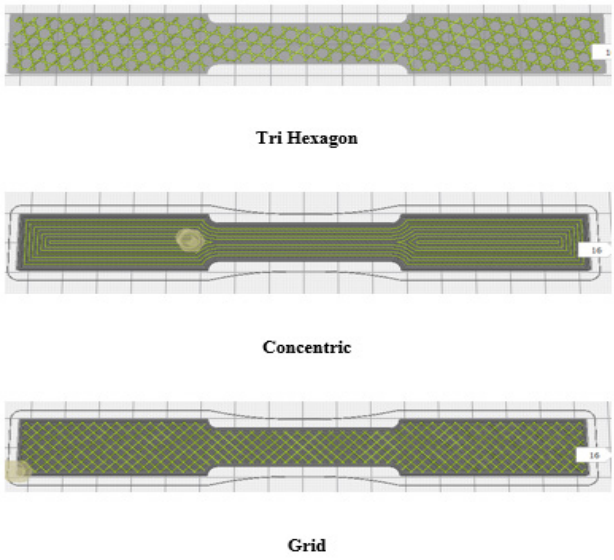

FIGURE 3. Internal structures

OBJECTIVES

The objectives of this project are as follows:

1. To evaluate existing or current manufacturing FDM processes in detail.

2. To analyze the impact of different input variables on mechanical properties through experiments.

3. To optimize input parameters through response surface methodology.

4. To validate experimental results with standard research papers.

DESIGN OF EXPERIMENT

In this study, Full Factorial Method is selected. This method is taken as per the guide's recommendation and is necessary. In a factorial design method, all possible combination of the level of the factor is investigated in each replication. A full factorial design of the experiment (DOE) measures the response of every possible combination of factors and factor levels. These responses are analyzed to provide information about every main and interaction effect. A full factorial DOE is practical when fewer than five factors are being investigated. This method is so balanced as well as orthogonal because it arranges all the parameters equally.

Here, the factors selected are three for the experiment, the number of parameters is also three and considering at three different levels, total 27 numbers of experiments were done. For the experimental design, the software Minitab version 17.0 was used.

Table1. Input Parameter Block for Design of Experiment

Parameter	Range		
Layer Thick (mm)	0.05	0.1	0.15
Nozzle Temp (◦c)	220	230	240
Profile	G	C	TH

Where G – Grid C – Concentric TH – Tri Hexagon

After giving Input values in the software windows, experimental design combinations in Table 1. as per run order are given below:

Experiments are performed in the college workshop. The experiment is conducted Ultimeker^{2+} 3D printer. First of all, the design was conducted in CURA software then taken the parameters such as layer thickness, nozzle temperature, and internal profile after the parameter it was conducted into the 3D printer after printed sample

SURFACE ROUGHNESS MEASUREMENT

After the key way to complete 3D Printed Simple, the roughness of the keyway is measured by taking an average of three readings on one keyway by the Mitutoyo surface roughness calibrated instrument.

After experimenting with different parameters by using calculated MMR and surface roughness for 27experiments

TENSILE TEST MEASUREMENT

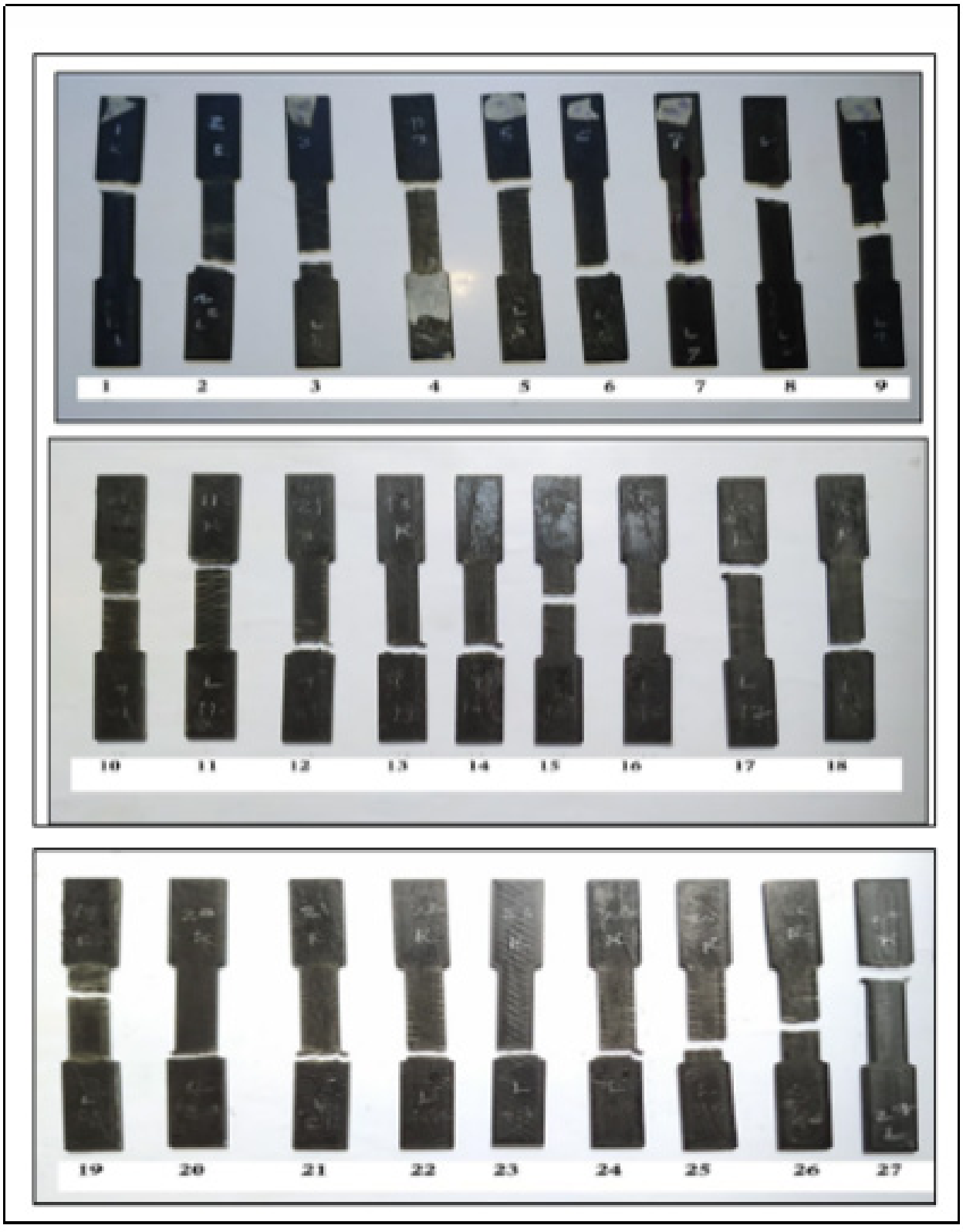

FIGURE 4. Tensile Tested Specimen

After the experiment considering tensile test observations Results show in Table 2.

TABLE 2. Results of Analysis and Optimum Value

Sr. No.	Layer Thick (mm)	Nozzle Temp ()	Profile	T. S. (MPa)	Avg. Surface Roughness (μm)
1	0.05	220	G	26.8	17.88
2	0.05	220	C	23.31	18.41
3	0.05	220	TH	28.93	18.3
4	0.05	230	G	27.75	18.18
5	0.05	230	C	28.73	17.62
6	0.05	230	TH	29.64	18.51
7	0.05	240	G	26.82	16.66
8	0.05	240	C	26.14	18.58
9	0.05	240	TH	29.02	17.61
10	0.1	220	G	26.81	17.19
11	0.1	220	C	28.11	17.91
12	**0.1**	**220**	**TH**	**29.7**	**18.37**
13	0.1	230	G	27.29	18.39
14	0.1	230	C	28.37	18.83
15	0.1	230	TH	26.56	18.68
16	0.1	240	G	27.4	17.23
17	0.1	240	C	28.35	18.68
18	0.1	240	TH	25.23	17.26
19	0.15	220	G	19.78	18.35
20	0.15	220	C	24.95	19.42
21	0.15	220	TH	23.66	17.12
22	0.15	230	G	19.03	18.33
23	0.15	230	C	28.98	18.36
24	0.15	230	TH	25.35	18.49
25	**0.15**	**240**	**G**	**24.38**	**15.86**
26	0.15	240	C	25.49	15.89
27	0.15	240	TH	24.07	16.61

RESULTS & DISCUSSION

The design of experiments along with the testing results of tensile strength and surface roughness was used to generate regression Analysis of input parameters to optimize the output parameter using Minitab 17. The step-wise creates a D.O.E. list of all the experimental data along with the results of testing of the output parameter. The Surface roughness had been taken by the calibrated instrument.

REGRESSION ANALYSIS: TENSILE VERSUS LAYER THICKNESS, NOZZLE TEMPERATURE, PROFILE

TABLE 3. Analysis of Variance of Tensile Strength

Source	DF	Seq. SS	Contribution	Adj. SS	Adj. MS	F-Value	P-Value
Layer Thickness	2	74.453	38.98%	74.453	37.226	35.47	0.001
Nozzle Temperature	2	23.998	12.56%	23.998	11.999	11.43	0.005
Profile	2	6.512	3.41%	6.512	3.256	3.1	0.101

continue ...

... cont.

Layer Thick*Nozzle Temp	4	30.866	16.16%	30.866	7.717	7.35	0.009
Layer Thick*Profile	4	17.567	9.20%	17.567	4.392	4.18	0.041
Nozzle Temp*Profile	4	29.207	15.29%	29.207	7.302	6.96	0.01
Error	8	8.397	4.40%	8.397	1.05		
Total	26	191.002	100.00%				

DF - degrees of freedom, SS - the sum of squares, MS - mean squares (Variance), F-ratio of variance of a source to the variance of error, $P < 0.05$ - determines the significance of a factor at 95% confidence level at Table 3.

TABLE 4. Model Summary of Tensile Strength

S	R-sq	R-sq(Adj.)	PRESS	R-sq(Pred.)
1.0245	95.60%	85.71%	95.6453	49.92%

R^2– The percentage of R-square shows how much confidence one can be about the predictions made by this model which is not observed and within the range, for this model the value of percentage of Table 4. in R-square for tensile strength is 95.60%, then one can be 96% confident that the prediction is right. There is only a 4% margin for error.

REGRESSION ANALYSIS: SURFACE ROUGHNESS VERSUS LAYER THICKNESS, NOZZLE TEMPERATURE, PROFILE

TABLE 5. Analysis of Variance Surface Roughness

Source	DF	Seq. SS	Contribution	Adj. SS	Adj. MS	F-Value	P-Value
Layer Thickness	2	50.597	46.94%	50.5972	25.2986	17.28	0.001
Nozzle Temperature	2	17.097	15.86%	17.0971	8.5485	5.84	0.027
Profile	2	0.051	0.05%	0.0511	0.0256	0.02	0.983
Layer Thick*Nozzle Temp	4	21.737	20.17%	21.7369	5.4342	3.71	0.054
Layer Thick*Profile	4	2.718	2.52%	2.7178	0.6794	0.46	0.761
Nozzle Temp*Profile	4	3.865	3.59%	3.8652	0.9663	0.66	0.637
Error	8	11.715	10.87%	11.7154	1.4644		
Total	26	107.781	100.00%				

DF - degrees of freedom, SS - the sum of squares, MS - mean squares (Variance), F-ratio of variance of a source to the variance of error, $P < 0.05$ - determines the significance of a factor at 95% confidence level at Table 5.

TABLE 6. Model Summary Surface Roughness

S	R-sq	R-sq (adj)	PRESS	R-sq (pred)
1.21014	89.13%	64.67%	133.446	0.00%

R^2– Prediction – This percentage shows how much the model is valid behind its range. If the percentage is 70%, then the model can be applied to the data behind its input range and one can be 70% sure that the results are valid.

The optimum values of input and output parameters are as follows:

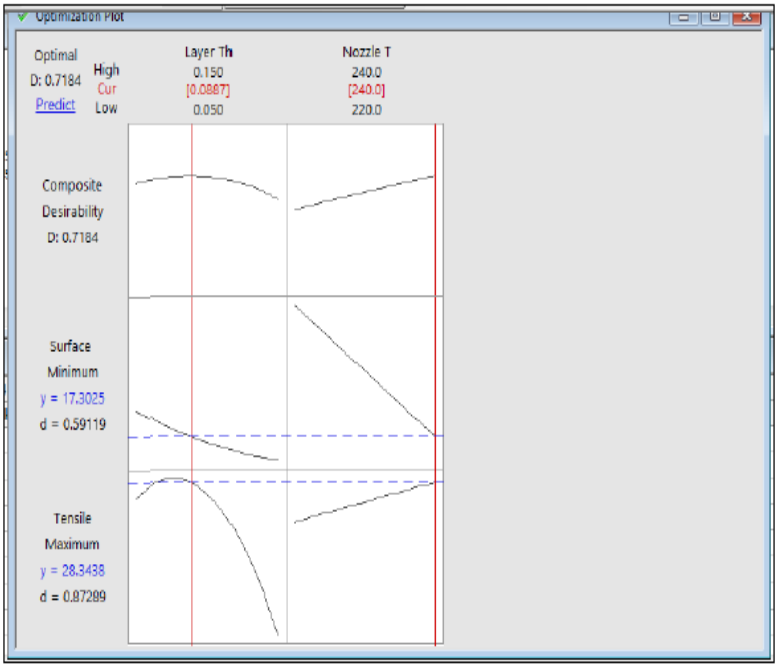

FIGURE 5. Result of Optimization

Optimum Input Parameters:

- Nozzle Temperature – 220, 230, 240 (° C)
- Profile – G, C, TH

Optimum Output Parameter

- Tensile strength = 28.34 MPa
- Surface Roughness = 17.30 µm

The optimum values of input and output parameters achieved from optimization are already included in DOE and experiments are already done. Therfore, the validated results are as follows:

From the Figure 5 result can be taken considering input parameters such as layer thickness and nozzle temperature without putting parameters such as surface roughness and tensile strength of regression analysis

Here run order 12 as shown in table 2. is the optimum value of parameters which is obtained by optimization in Minitab and it's already been tested.

Here run order 25 as shown in table. 2 is the optimum value of parameters which is obtained by optimization in Minitab and it's already been tested.

It is evident from the above-described comparison that the results obtained from the experimentation are very accurate and precise with the results of the software Table 7.

TABLE 7. Comparison of Optimum Result

Parameter	Minitab Result	Experimental Result	Error Between Minitab and Experimental Results (%)
Tensile Strength	28.34 MPa	29.22MPa	3.01 %
Surface Roughness	17.30 µm	15.86µm	

ANALYSIS OF OBTAINED RESULTS

TENSILE STRENGTH

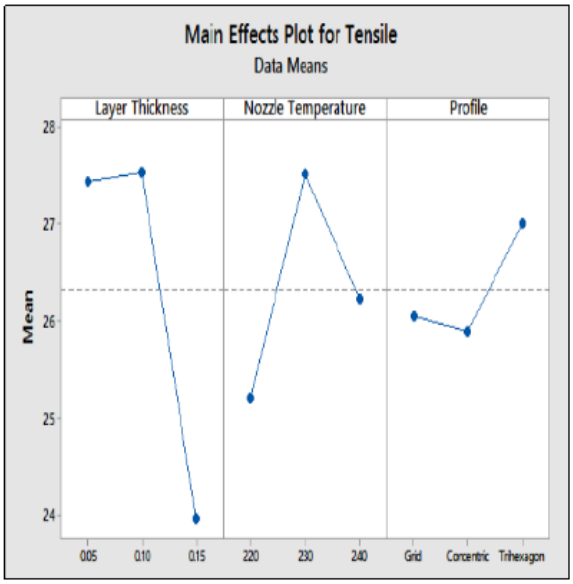

FIGURE 6. Main Effect Plot for Tensile strength

Figure 6 shows that tensile strength decreases with an increase in layer thickness, thus it is inversely proportional to layer thickness. And it has a major effect on tensile strength. Tensile strength increases with decreases in nozzle temperature; thus, it is directly proportional to nozzle temperature. It has equally effective on tensile strength like layer thickness. Tensile strength increases within the profile; thus, it is inversely proportional to the profile. It is also effective on tensile strength.

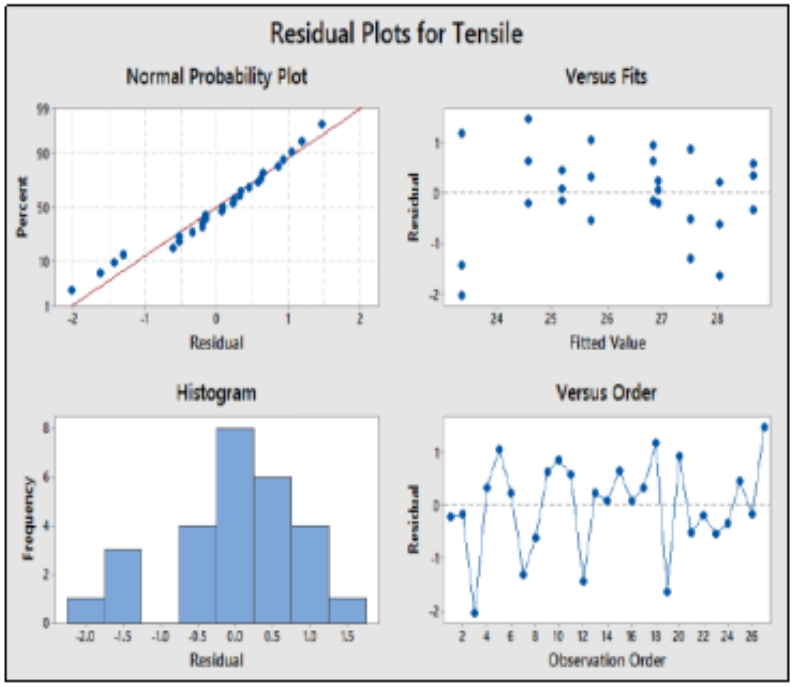

FIGURE 7. Residual Plots for Tensile strength

Figure 7 shows that from the above graphs, it can be observed that the observed values of distortion and the predicted values are having good similarity. From Figure 7 the normal probability plot shows that the obtained results are very close to the straight line, it can be said that the observed data of tensile strength is normally distributed around the mean line. Figure 7 represents residual versus the fitted values. The observations range from 21 to 29 Mpa. From the graph, it can be observed that there is no particular pattern generated for the results. Hence, the observations are almost equally distributed around the residual mean line.

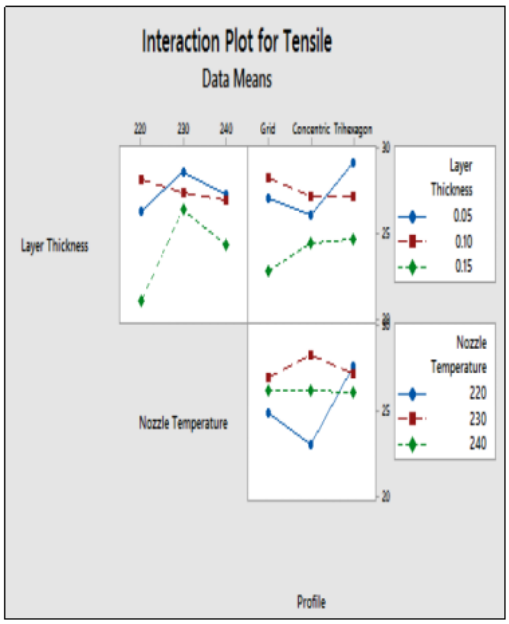

FIGURE 8. Interaction Plots for Tensile strength

Figure 8 shows the Interaction effect of Tensile strength on various parameters shown in Figure 11 it's seen that the optimum value of tensile strength can be obtained at nozzle temperature 230°C, layer thickness 0.1 mm, and concentric profile. It also shows that from the grid, concentric, and tri hexagons profile the tensile strength is increased with 220°C nozzle temperature. From the grid, concentric, and tri hexagon profile the tensile strength is first increased and then decreases with 230°C nozzle temperature. And from the grid, concentric, and tri hexagon profile the tensile strength almost remains the same with 230 °C and 240°C nozzle temperatures, while it increased at 220°C.

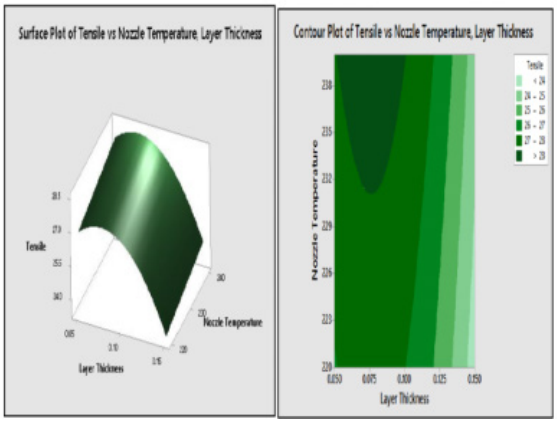

FIGURE 9. Surface Plot & Contour Plot for Tensile vs. Layer thickness & Nozzle temperature

Figure 9 shows the surface plot and contour plot for Tensile. FIGURE 9 shows that a tensile gradually increased after 0.10-layer thickness continuously decreases. In Figure 9 contour plot shows that 0.05 mm to 0.1 mm layer thickness and nozzle temperature 230°C to 240°C maximum value of tensile strength gets the result.

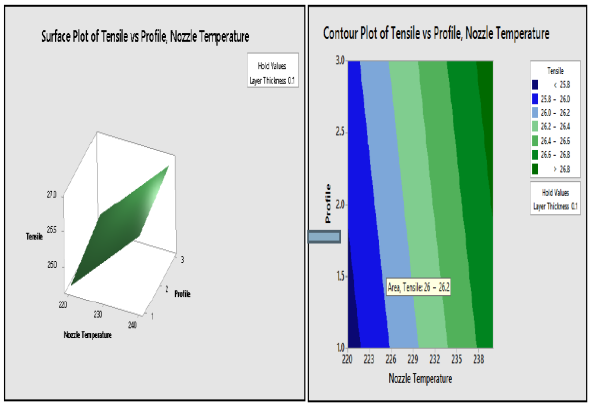

FIGURE 10. Surface Plot & Contour Plot for Tensile vs. Nozzle Temperature & Profile

Figure 10shows that a tensile value will be directly impropriation to tensile strength. In Figure 10 contour plot shows that considering tri hexagon profile with high nozzle temperature tensile strength maximum.

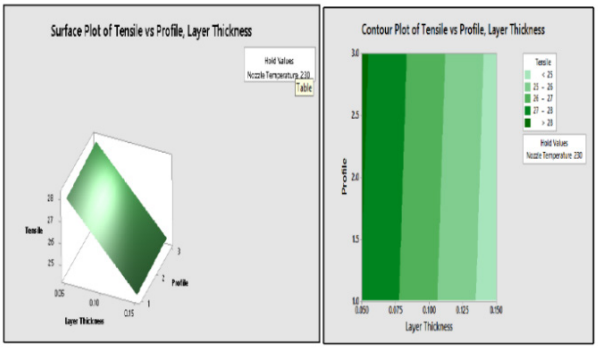

FIGURE 11. Surface Plot & Contour Plot for Tensile vs. Layer thickness & Profile

Figure 11 shows that a tensile strength value can be seen that layer thickness is inversely profanation to tensile strength, in Figure 11 contour plot shows that nozzle temperature and profile with considering minimum layer thickness and tri hexagon profile. Tensile strength is maximum.

SURFACE ROUGHNESS

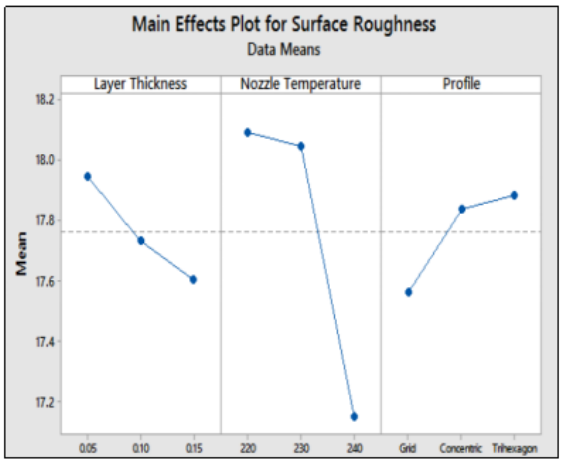

FIGURE 12. Main Effect Plot for Surface Roughness

Figure 12 shows that Surface Roughness decreases with an increase in layer thickness, thus it is inversely proportional to layer thickness. And it has a major effect on Surface Roughness. At the initial level Surface Roughness slightly decreases with an increase in nozzle temperature, then it is suddenly decreased. Surface Roughness increases within the profile and is maximum with a tri-hexagon profile.

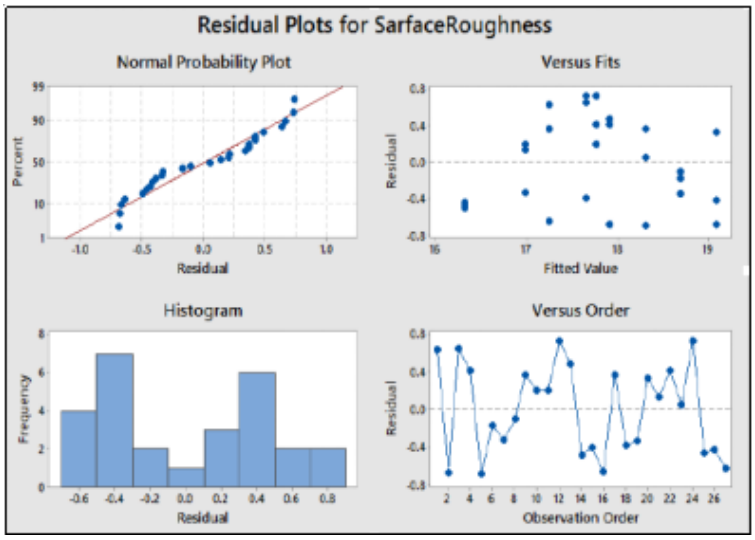

FIGURE 13. Residual Plots for Surface Roughness

Figure 13 from the above graphs, it can be observed that the observed values of distortion and the predicted values are having good similarity. From FIGURE13 the normal probability plot shows that the obtained results are very close to the straight line, it can be said that the observed data of surface roughness is normally distributed around the mean line. FIGURE 13 represents residual versus the fitted values. The observations range from 15 to 19 µm. From the graph, it can be observed that there is no particular pattern generated for the results. Hence, the observations are almost equally distributed around the residual mean line.

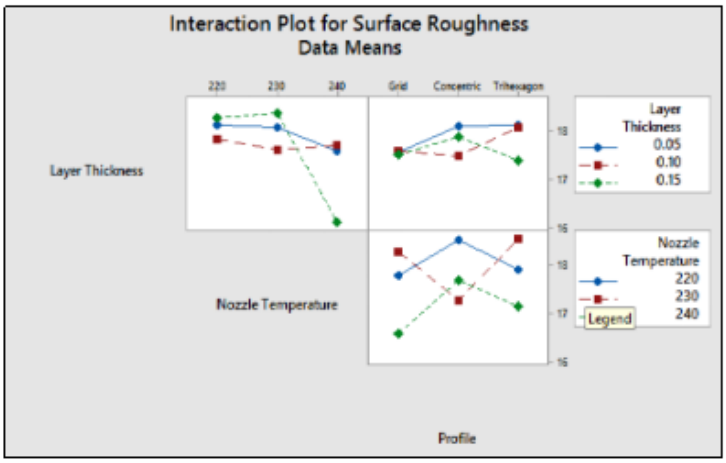

FIGURE 14. Interaction Plots for Surface Roughness

The interaction effect of surface roughness on various parameters is shown in Figure 14 it's seen that the optimum value of surface roughness can be obtained at nozzle temperature 230°C, layer thickness 0.15 mm, and concentric profile. It also shows that with 220°C and 240°C nozzle temperatures having the same value and surface roughness is minimum.

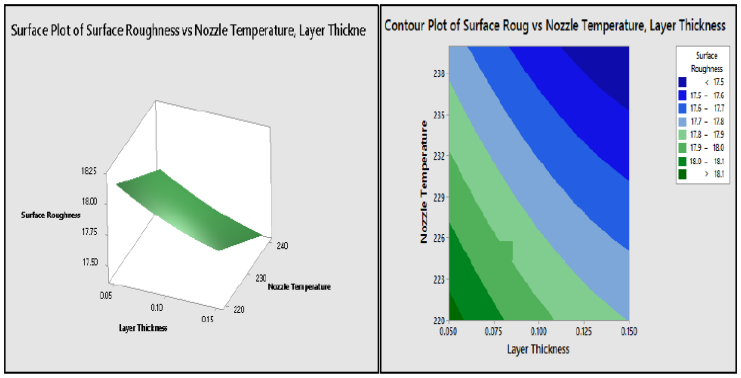

FIGURE 15. Surface Plot & Contour Plot for Surface Roughness vs. Layer thickness & Nozzle temperature

Figure 15 shows the surface plot and contour plot for Surface Roughness. It shows that a surface roughness value will be decreased to decreases in layer thickness and nozzle temperature. The contour plot shows that 0.1 mm to 0.15 mm layer thickness and nozzle temperature 230°C to 240°C minimum value of surface roughness get the result.

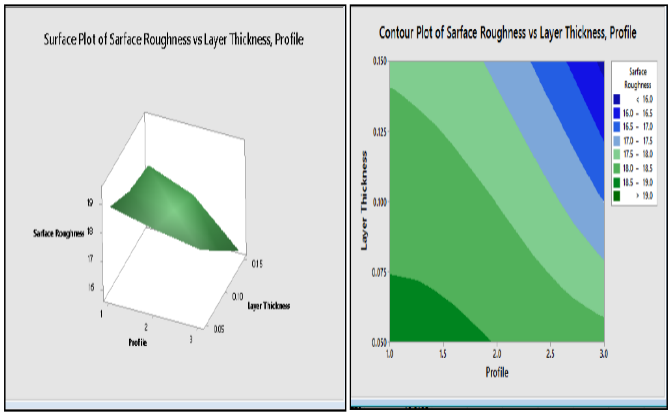

FIGURE 16. Surface Plot & Contour Plot for Surface Roughness vs. Layer thickness & Profile

Figure 16 shows that a surface roughness value will be decreased to decreases in layer thickness and Profile. In Figure 16 contour plat shows that 0.1 mm to 0.15 mm layer thickness and Profile tri hexagon minimum value of surface roughness gets the result.

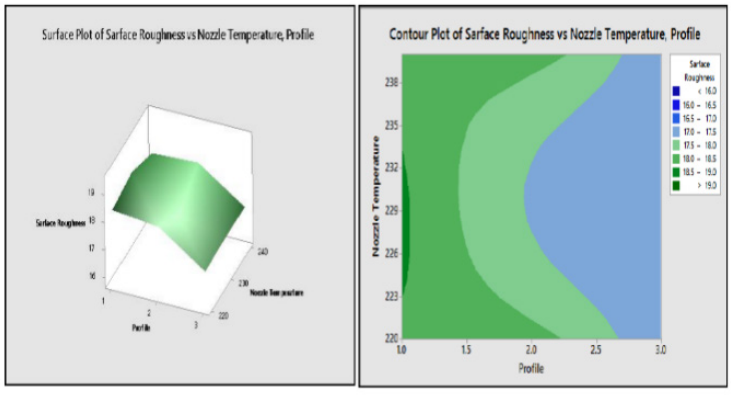

FIGURE 17. Surface Plot & Contour Plot for Surface Roughness vs. Nozzle temperature & Profile

Figure 17 show that the surface roughness value will be both are same in Nozzle Temperature and Profile. In Figure 20 contour plat shows that nozzle temperature and profile both are the same value of surface roughness to get the result.

CONCLUSION

Based on the experiment results presented and discussed, the following conclusion is drawn on the effect of layer thickness, nozzle temperature, and profile. The experiment is done by ASTM D638 – 14 ABS with Ultimaker^{+2}3D Printer by considering DOE and Regression Analysis. It can be concluded that with Layer thickness 0.1 mm, Nozzle temperature 220°C and Tri Hexagon profile at the maximum Tensile strength 29.70 MPa is obtained. It can be concluded that with a Layer thickness of 0.15 mm, Nozzle temperature of 240°C and with 17.6 grid profile pattern, the minimum Surface Roughness of 15.86 µm is obtained. With 0.1mm layer thickness, Nozzle Temperature 220°C and tri hexagon Profile optimum manufacturing time is obtained hence concentric profile is recommended. It can be observed that considering the Tri hexagon profile, less material weight with high tensile strength was obtained. The results showed that printing parameters have a very important role in surface roughness. In this work considering the Grid profile, justify minimum surface roughness.

The different applications with various printing parameters and materials will contribute to the development of engineering design applications. Enhance, different surface characteristics of parts produced by 3D printers will be understood easily. This work is considered ABS material and can be made for the development of a product using different materials. This work is considered with Grid, concentric, and tri hexagons that can be made for the development of a product using different mechanical profiles.

ACKNOWLEDGEMENT

We would to thank GTU, Ahmedabad and Atmiya Institute of Technology & Science Rajkot, India for supporting this study.

DECLARATION OF COMPETING INTEREST

None.

REFERENCES

Akessa, A. D., Lemu, H. G., & Gebisa, A. W. 2017. Mechanical property characterization of additive manufactured ABS material using design of experiment approach. In *ASME International Mechanical Engineering Congress and Exposition.* 2017, (Vol. 58493, p. V014T07A004).

Angrish, A. 2014. A critical analysis of additive manufacturing technologies for aerospace applications. In *2014 IEEE Aerospace Conference* : 1-6

Anoosha, N. M., Sachin, B., Hemanth, B. R. & Pavan Kumar. 2018. Tensile test & FEM Analysis of ABS material using FDM Technique. *International Journal of Innovation Research in Science Engineering and Technology* 7(6): 6658 - 6663

Bagsik, K. I., Gebisa, A. W., & Lemu, H. G. 2018. Mechanical properties of ULTEM 9085 material processed by fused deposition modeling. *Polymer Testing* 72: 335-347

Basavaraj, C. K., & Vishwas, M. 2016. Studies on the effect of fused deposition modeling process parameters on ultimate tensile strength and dimensional accuracy of nylon. In *IOP conference series: materials science and engineering.* 2016, (Vol. 149)

Bauer, M., & Kulinsky, L. 2018. Fabrication of a lab-on-chip device using material extrusion (3D printing) and demonstration via Malaria-Ab ELISA. *Micromachines* 9(1).

CH, V. M., & Yeole, S. N. 2016. Relative Studies on

ASTM D638 Type–IV Specimens 3D Printed using ABS.

Christiyan, K. J., Chandrasekhar, U., & Venkateswarlu, K. 2016. A study on the influence of process parameters on the Mechanical Properties of 3D printed ABS composite. In *IOP Conference Series: Materials Science and Engineering* 114(1): 012109.

Durgun, I. & Ertan, R. 2014. Experimental investigation of FDM process for improvement of mechanical properties and production cost. *Rapid Prototyping Journal*.

Farbman, D., & McCoy, C. 2016. Materials testing of 3D Printed ABS and PLA samples to guide mechanical design. In *International Manufacturing Science and Engineering Conference.* American Society of Mechanical Engineers. Vol. 49903: V002T01A015.

Farbman, D., & McCoy, C. Materials testing of 3D printed ABS and PLA samples to guide mechanical design. In *International Manufacturing Science and Engineering Conference* 2016, American Society of Mechanical Engineers. (Vol. 49903): V002 To 1A015

Farzadi, A., Solati-Hashjin, M., Asadi-Eydivand, M., & Osman, N. A. A. 2014. Effect of layer thickness and printing orientation on mechanical properties and dimensional accuracy of 3D printed porous samples for bone tissue engineering. *PloS one* 9(9).

Galantucci, L. M., Bodi, I., Kacani, J., & Lavecchia, F. 2015. Analysis of dimensional performance for a 3D open-source printer based on fused deposition modeling technique. *Procedia Cirp* 28: 82-87.

Galatas, A., Hassanin, H., Zweiri, Y., & Seneviratne, L. 2018. Additive manufactured sandwich composite/ ABS parts for unmanned aerial vehicle applications. *Polymers* 10(11): 1262.

Gebisa, A. W., & Lemu, H. G. 2019. Influence of 3D printing FDM process parameters on the tensile property of ULTEM 9085. *Procedia Manufacturing* 30: 331-338.

Joshi, S. C., & Sheikh, A. 2015. A 3D printing in Aerospace and its long-term sustainability. *Virtual and Physical Prototyping* 10(4): 175-185.

Khan, S. F., Zukhi, M. M., Zakaria, H., & Saad, M. A. M. 2019. Optimize 3D printing parameter on the mechanical performance of PLA-wood fused filament fabrication. In *IOP Conference Series: Materials Science and Engineering* 670(1).

Knoop, F., Schoeppner, V., & Knoop, F. C. 2015. Mechanical and thermal properties of FDM parts manufactured with polyamide 12. In *Proceedings of the 26th Annual International Solid Freeform Fabrication Symposium—an Additive Manufacturing Conference, Austin, TX, USA*:10-12

Kovan, V., Tezel, T., Topal, E. S., & Camurlu, H. E. 2018. Printing parameters affect on surface characteristics of 3D-printed PLA materials. *Machines. Technologies. Materials.* 12(7):266-269.

Kucewicz, M., Baranowski, P., Małachowski, J., Popławski, A., & Płatek, P. 2018. Modelling, and characterization of 3D printed cellular structures. *Materials & Design* 142:177-189.

Mohamed, O. A., Masood, S. H., & Bhowmik, J. L. 2017. Experimental investigation of time-dependent mechanical properties of PC-ABS prototypes processed by FDM additive manufacturing process. *Materials Letters* 193:58-62.

Mohamed, O. A., Masood, S. H., & Bhowmik, J. L. 2016. Experimental investigations of process parameters influence rheological behavior and dynamic mechanical properties of FDM manufactured parts. *Materials and Manufacturing Processes* 31(15):1983-1994.

Mohan, N., Senthil, P., Vinodh, S., & Jayanth, N. 2017. A review of composite materials and process parameters optimization for the fused deposition modeling process. *Virtual and Physical Prototyping* 12(1): 47-59.

Ngo, T. D., Kashani, A., Imbalzano, G., Nguyen, K. T., & Hui, D. 2018. Additive manufacturing (3D printing): A review of materials, methods, applications, and challenges. *Composites Part B: Engineering* 143: 172-196.

Paleti, B. M., Navuri, K., Eswara Kumar, A., Teja, P. V. S. & Vaddeswaram, A. 2017. Analysis of effect of internal structures on tensile strength of the fdm parts. *International Journal of Pure and Applied Mathematics* 115(6): 123-131.

Paleti, B. M., Navuri, K., Eswara Kumar, A., Teja, P. V. S., & Vaddeswaram, A. 2017. Effect of internal structures on compressive strength of the FDM parts. *International Journal of Pure and Applied Mathematics* 115(6): 139-146.

Pollard, D., Ward, C., Herrmann, G., & Etches, J. 2017. The manufacture of honeycomb cores using Fused Deposition Modeling. *Advanced Manufacturing: Polymer & Composites Science* 3(1):21-31.

Qattawi, A., Alrawi, B., & Guzman, A. 2017. Experimental optimization of fused deposition modeling processing parameters: a design-for-manufacturing approach. *Procedia Manufacturing* 10:791-803.

Rajpurohit, S. R., & Dave, H. K. 2019. Analysis of tensile strength of a fused filament fabricated PLA part using an open-source 3D printer. *The International Journal of Advanced Manufacturing Technology* 101(5-8): 1525-1536.

Raney, K., Lani, E., & Kalla, D. K. 2017. ABS parts manufactured by fused deposition modeling process. *Materials Today: Proceedings* 4(8): 7956-7961.

Sandeep, D. C., & Chhabra, D. 2017. Comparison and analysis of different 3d printing techniques. *International Journal of Latest Trends in Engineering and Technology* 8(4-1): 264-272.

Sathyaseelan, P., Thamaraikannan, M., Irfan Ahmed I. Mr. Nandinerav and aBheemaiah. 2018. Tensile and hardness characterization of rapid prototyped, abs prototypes. *International Journal of Mechanical Engineering and Technology* 8(8): 499 – 510.

Sood, A. K., Ohdar, R. K., & Mahapatra, S. S. 2010. Parametric appraisal of mechanical property of fused deposition modeling processed parts. *Materials & Design* 31(1):287-295.

Stopka, M., Kohar, R., Gramblička, S., & Madaj, R. 2017. Dynamical Analysis of 3D Printer's Powertrain. *Procedia Engineering* 192: 845-850.

Torres, J., Cole, M., Owji, A., DeMastry, Z., & Gordon, A. P. 2015. An approach for mechanical property optimization of fused deposition modeling with polylactic acid via the design of experiments. *Rapid Prototyping Journal*. 2016

Torres, J., Cotelo, J., Karl, J., & Gordon, A. P. Mechanical property optimization of FDM PLA in shear with multiple objectives. *Jom* 67(5): 1183-1193.

Uz Zaman, U. K., Boesch, E., Siadat, A., Rivette, M., & Baqai, A. A. 2019. Impact of fused deposition modeling (FDM) process parameters on strength of built parts using Taguchi's design of experiments. *The International Journal of Advanced Manufacturing Technology* 101(5-8) :1215-1226.

Wang, W. M., Zanni, C., & Kobbelt, L. 2016. Improved surface quality in 3D printing by optimizing the printing direction. *Computer Graphics Forum* 35(2): 59-70.

Wittbrodt, B., & Pearce, J. M. 2015. The effects of PLA color on material properties of 3-D printed components. *Additive Manufacturing* 8:110-116.

Yang, Y., Li, L., & Zhao, J. 2019. Mechanical property modeling of photosensitive liquid resin in stereo lithography additive manufacturing: Bridging degree of cure with tensile strength and hardness. *Materials & Design* 162:418-428.

Yubo, T. A. O., Peng, L. I., & Ling, P. A. N. 2019. Improving tensile properties of polylactic acid by adjusting printing parameters of open-source 3d printers. *Materials Science* 26(1):83-87.

Zekavat, A. R., Jansson, A., Larsson, J. & Pejryd, L. 2019. Investigating the effect of fabrication temperature on mechanical properties of fused deposition modeling parts using X-ray computed tomography. *The International Journal of Advanced Manufacturing Technology* 100(1-4):287-296.